Symmetry breaking in dipolar matter-wave solitons in dual-core couplers

Yongyao Li,[1,2,3] Jingfeng Liu,[2] Wei Pang,[4] and Boris A. Malomed[1,*]

[1]*Department of Physical Electronics, Faculty of Engineering, School of Electrical Engineering, Tel Aviv University, Tel Aviv 69978, Israel*

[2]*Department of Applied Physics, South China Agricultural University, Guangzhou 510642, China*

[3]*Modern Educational Technology Center, South China Agricultural University, Guangzhou 510642, China*

[4]*Department of Experiment Teaching, Guangdong University of Technology, Guangzhou 510006, China*

(Received 15 October 2012; published 7 January 2013)

We study the effects of spontaneous symmetry breaking (SSB) in solitons composed of a dipolar Bose-Einstein condensate trapped in a dual-core system with dipole-dipole interactions (DDIs) and hopping between the cores. Two realizations of such a matter-wave coupler are introduced: weakly and strongly coupled. The former is based on two parallel pipe-shaped traps, whereas the latter is represented by a single pipe sliced by an external field into parallel layers. The dipoles are oriented along the axes of the pipes. In these systems, the dual-core solitons feature SSB of the supercritical and subcritical types, respectively. Stability regions are identified for symmetric and asymmetric solitons and nonbifurcating antisymmetric solitons, as well as for symmetric flat states, which may also be stable in the strongly coupled system due to competition between the attractive and repulsive intracore and intercore DDIs. The effects of the contact interactions are considered too. Collisions between moving asymmetric solitons in the weakly symmetric system feature an elastic rebound, a merger into a single breather, and passage accompanied by excitation of intrinsic vibrations of the solitons for small, intermediate, and large collision velocities, respectively. A $\mathcal{PT}$-symmetric version of the weakly coupled system is considered briefly, which may be relevant for matter-wave lasers. Stability boundaries for $\mathcal{PT}$-symmetric and -antisymmetric solitons are identified.

DOI: 10.1103/PhysRevA.87.013604 PACS number(s): 03.75.Lm, 42.65.Tg, 47.20.Ky, 05.45.Yv

I. INTRODUCTION

Studies of Bose-Einstein condensates (BECs) made of dipolar atoms or molecules have produced a great deal of fascinating experimental and theoretical results, which have been summarized in Refs. [1,2] and [2,3], respectively. The continuation of the work in this direction has yielded new remarkable findings such as the prediction of various pattern-formation mechanisms [4,5] (which share some features with the formation of patterns in ferrofluids [6]), analysis of the stability of the dipolar BEC trapped in optical-lattice (OL) potentials [7], analysis of the roton instability [5,8], and the possibility of the Einstein–de Haas effect [9]. Important experimental achievements, which offer new perspectives for studies of dipole-dipole interactions (DDIs) in atomic condensates, are the creation of BECs in dysprosium [10] and erbium [11]. Parallel to that, essential results have been obtained for degenerate quantum gases of dipolar fermions [3,12].

In addition to their own physical significance, dipolar condensates may also be used as quantum simulators [13,14] representing other physical media where nonlocal nonlinearities play a fundamental role. These include the heating and ionization of plasmas [15]; nonlinear optics of nematic liquid crystals [16], of waveguides sensitive to temperature variations [17], and of semiconductor cavities [18]; BECs with long-range interactions induced by laser illumination [19]; and others settings.

An interesting ramification of the study of collective nonlinear modes in the dipolar BEC is the prediction of solitons (which have not yet been reported in experimental works). In effectively one-dimensional (1D) traps, solitons have been analyzed in both continual [20] and discrete [21] settings, the latter corresponding to the fragmentation of the BEC by a deep OL. In a similar form, 1D solitons supported by the attractive DDIs were predicted in the Tonks-Girardeau gas of dipolar hard-core bosons [22]. Taking into account the 3D structure of the quasi-1D cigar-shaped traps, the solitons, including ones with embedded vorticity (cf. similar modes introduced earlier in the context of BECs with local interactions [23]), were further studied in Ref. [24] and gap solitons in a similar setting, but including an OL potential, were considered as well [25]. In the 2D system, discrete fundamental solitons and solitary vortices with long-range DDIs between sites of the lattice can be constructed easily [26]. In the continual 2D model, fundamental [27] and vortical [28] solitons were constructed in the isotropic setting, assuming that the sign of the DDI could be reversed from repulsion to attraction by means of a rapidly oscillating ac field [29]. Two-dimensional fundamental and vortex solitons supported by a trapping potential were introduced in Ref. [30].

Without reversing the DDI sign, stable 2D anisotropic solitons, corresponding to the in-plane polarization of dipoles, were constructed in Ref. [31] by means of the variational approximation and systematical numerical simulations. The variational approximation for 2D solitons supported by the DDI was analyzed in Ref. [32] and a rigorous proof of the existence of such solitons was provided too [33]. Also studied were more complex situations, such as the formation of a multisoliton patterns as a result of the development of the modulational instability of an extended state [34].

The long-range character of the DDI makes it possible to consider interactions between condensate layers trapped in parallel planar waveguides. The DDI couples them by nonlinear forces even in the absence of hopping (tunneling)

*malomed@post.tau.ac.il

of atoms across gaps separating the layers [5] (the isolation of parallel layers can be provided by a strong OL field whose axis is perpendicular to the layers [35]). This nonlocal interaction gives rise to indirect scattering of 2D solitons moving in the separated layers [36] and the formation of bound states of such solitons [37]. The creation of multisoliton filaments and checkerboard crystals in a multilayered stack was predicted too [38].

The model of nonlocal DDIs between parallel layers considered in Refs. [5,36–38] did not take into regard the hopping (tunneling of atoms, also known as linear coupling) between the layers. In contrast, models of dual-core couplers, with intrinsic local nonlinearity acting in both cores, were studied in detail in terms of optics and matter waves, starting from the analysis of the spontaneous symmetry breaking (SSB) of cw (i.e., uniform) states in dual-core optical fibers with the cubic and more general forms of the intracore nonlinearity. In that system, the linear coupling is caused by the overlap of the evanescent field, originating from each core, with the parallel one. The SSB happens in the dual-core fiber, as a result of the interplay of the linear coupling and intrinsic nonlinearity, with the increase of the total power of the cw beam. The analysis of the SSB was extended, in full detail, to temporal and spatial solitons [39,40] and to optical domain walls [41]. The SSB effects were also studied for solitons in dual-core fiber Bragg gratings [42], in two-tier waveguiding arrays (for discrete solitons) [43], in parallel-coupled waveguides with the quadratic (second-harmonic-generating) [44] and cubic-quintic (CQ) [45] nonlinearities, and for dissipative solitons in linearly coupled CQ complex Ginzburg-Landau equations [46]. Recently, a similar analysis was developed for the SSB of solitons in $\mathcal{PT}$-symmetric couplers, with mutually balanced loss and gain (and identical cubic nonlinearities) acting in the two cores [47,48]. Unlike the above-mentioned settings, in the latter case the SSB destroys symmetric solitons rather than replacing them by stable asymmetric ones. The linear coupling in optics may also represent the mutual interconversion of two polarizations of light in twisted fibers (which, in particular, are used in the so-called rocking filters) [49], twisted photonic-crystal fibers [50], and twisted fiber gratings [51] or the interconversion of two waves with different carrier frequencies caused by electromagnetically induced transparency [52].

Similar dual-core (double-well) settings, approximated by linearly coupled Gross-Pitaevskii equations (GPEs), were introduced for the mean-field wave functions describing a trapped BEC with local interactions [53]. A similar linear coupling accounts for the mutual interconversion in a mixture of two different atomic states induced by a resonant electromagnetic wave [54]. The linearly coupled GPEs were used to predict the shift of the miscibility-immiscibility transition in BEC or fermionic mixtures of two states connected by the linear interconversion [55] and the stabilization of 2D solitons against the collapse in a linearly coupled binary system with attractive and repulsive intracomponent interactions [56]. The SSB of matter-wave solitons trapped in 1D and 2D linearly coupled cores was analyzed in Ref. [53]. In the 1D situation, a more accurate description, which, nevertheless, yields similar results for the solitons' SSB, is provided by the two-dimensional GPE, which, instead of postulating two 1D wave functions in the two parallel cores with the linear exchange between them, introduces a single 2D wave function comprising both cores [57]. This includes the case when the cores are defined by nonlinear pseudopotentials (rather than by a linear trapping potential), i.e., local modulation of the self-attraction coefficient [58].

Although previous works analyzed many aspects of the SSB in dual-core cw and solitonic states, those works were dealing solely with local intrinsic nonlinearities. Only in a very recent paper [59] was a shift of the SSB transition of solitons in the coupler with nonlocal nonlinearity of the thermal type, typical of optical systems [17], considered. The analysis was performed for two opposite-limit cases, viz., the weak nonlocality characterized by a small correlation radius, which may be approximated by the first two terms of the expansion of the nonlocal cubic term, and the opposite limit of the infinite correlation radius, which corresponds to the two-component quasilinear model of accessible solitons [60].

The aim of the present work is to consider the SSB of solitons in the effectively 1D dual-core coupler filled by the dipolar condensate, which exhibits the interplay of the long-range DDIs and linear hopping between the quasi-1D cores. In particular, the DDIs act both inside the cores and between them, while the thermal nonlocality considered in Ref. [59] could not act across the gap separating the parallel waveguides. It is relevant to stress that in the absence of the longitudinal dimension, the double-well setting is not sufficient to exhibit the nonlocal character of the interactions in the dipolar condensate, the minimum necessary configuration being based on a set of three potential wells [61].

Two coupler configurations are considered here, as shown in Fig. 1. The first setting, presented in Fig. 1(a), is based on two identical condensate-trapping pipes of diameter b, separated by distance a. In this case, $b < a$ is implied, hence the system may be naturally called weakly coupled. The other setting is shown in Fig. 2(b), with the condensate loaded into a single pipe of diameter b, which is sliced into two parallel layers by a thin potential barrier of small thickness a. The barrier can be induced by a repulsive light sheet (blue shifted by one with respect to the atoms) [62]. The latter setting implies $b > a$ and will accordingly be referred to as a strongly coupled system. In either case, the dipoles are polarized along the pipes' axes, hence the DDIs are attractive inside the cores, which makes it possible to form solitons in each one [20].

In studying the SSB (the symmetry-breaking phase transition) in these settings, it is relevant to recall that there are two types of the SSB bifurcation, namely, subcritical and supercritical [63], which are tantamount to the phase transitions of the first and second kinds, respectively. In the subcritical situation, branches representing asymmetric modes emerge as unstable states at the bifurcation point, then go backward in the bifurcation diagram, and stabilize after turning forward. In the supercritical setting, the asymmetric branches emerge as stable at the bifurcation point and immediately continue forward.

The rest of the paper is organized as follows. In Sec. II we construct symmetric solitons in the two settings presented in Fig. 1 and then identify the SSB transitions to asymmetric solitons. Antisymmetric solitons and their stability are considered too (these solitons do not undergo any bifurcation).

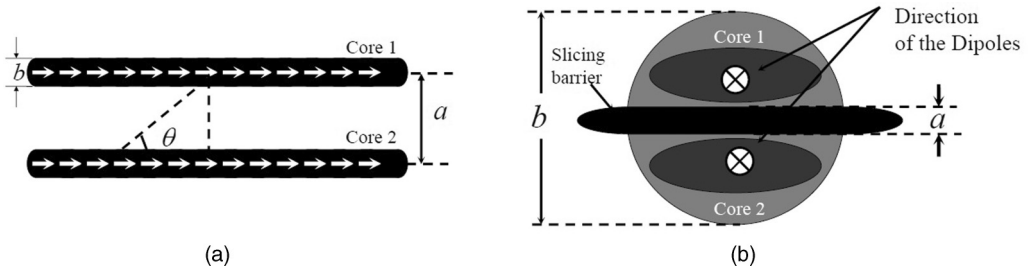

FIG. 1. (a) In the weakly coupled system, the dipolar condensates are trapped in parallel pipes of diameter b, separated by distance a. The arrows represent the orientation of the dipoles. (b) The strongly coupled system is shown by means of the cross-section image of the condensate trapped in the single pipe of diameter b, which is sliced by a repelling laser sheet into two layers, with effective separation a between them. The symbol $\otimes$ represents the orientation of the dipoles, which are perpendicular to the figure's plane.

Basic results for the stability of different modes are presented (including a flat state, which may also be stable in the strongly coupled system). The effects of the local (contact) nonlinearity on the SSB are considered too. In Sec. III we study collisions between moving asymmetric solitons. In Sec. IV a $\mathcal{PT}$-symmetric [64] extension of this system is briefly considered, which includes gain and loss applied to the two cores (similar to the $\mathcal{PT}$-symmetric coupler with the local nonlinearity introduced in Refs. [47,48]). The paper is summarized in Sec. V.

II. SYMMETRY-BREAKING BIFURCATION AND STABILITY OF SOLITONS

A. Coupled Gross-Pitaevskii equations

In the usual mean-field approximation [2,3], both dual-core settings introduced in Fig. 1 are described by the system of 1D linearly coupled GPEs for the wave functions in the two cores

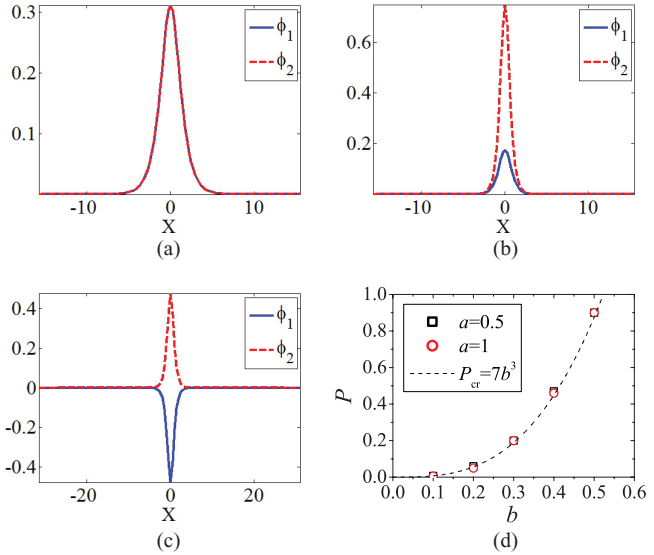

FIG. 2. (Color online) Examples of stable (a) symmetric, (b) asymmetric, and (c) antisymmetric solitons found in the weekly coupled system [see Fig. 1(a)] for $a = 1$, $b = 0.4$, and total norm (a) $P = 0.4$ and (b) and (c) $P = 0.6$. The antisymmetric solitons are stable below the boundary $P \approx 7b^3$, shown in the plane of (b, P) in (d), at different values of a.

ψ_1 and ψ_2. In scaled form, the equations are

$$i\frac{\partial \psi_n}{\partial t} = -\frac{1}{2}\frac{\partial^2 \psi_n}{\partial x^2} + g|\psi_n|^2\psi_n - \kappa\psi_{3-n} - G_{\rm DD}\psi_n(x)\int_{-\infty}^{+\infty}\left[\frac{|\psi_n(x')|^2}{(b^2+|x-x'|^2)^{3/2}} - \frac{1}{2}\frac{(1-3\cos^2\theta)|\psi_{3-n}(x')|^2}{2(a^2+|x-x'|^2)^{3/2}}\right]dx', \quad (1)$$

where $n = 1,2$ and $\cos\theta = |x-x'|/(a^2+|x-x'|^2)^{1/2}$ [see Fig. 1(a)]. In this notation κ is the coupling parameter (hopping coefficient), g represents the local interaction (repulsive in the case of $g > 0$), and the orientation of the dipoles in Fig. 1 corresponds to $G_{\rm DD} > 0$, which implies the attraction between dipoles in the given core and repulsion between the cores for $\cos^2\theta < 1/3$. The first term in the integrand, which accounts for the intracore DDIs, is regularized by the transverse diameter b, which is an approximation sufficient for producing 1D solitons [20].

The solitons will be characterized by the total norm (proportional to the number of atoms in the condensate)

$$P \equiv P_1 + P_2 = \int_{-\infty}^{+\infty}(|\psi_1|^2 + |\psi_2|^2)dx.$$

To focus on SSB effects dominated by the DDI, we will first drop the local nonlinearity by setting $g = 0$ (in the experiment this can be done by means of the Feshbach resonance [65]); the effects of the contact interactions will be considered afterward. Then we scale the units to srt $\kappa \equiv 1$ and $G_{\rm DD} \equiv 1$, the remaining free parameters being a, b, and P (and g too, in the end).

Stationary solutions to Eq. (1) with chemical potential μ are sought in the usual form $\psi_{1,2}(x,t) = \exp(-i\mu t)\,\phi_{1,2}(x)$, with real functions $\phi_{1,2}(x)$. In particular, $\phi_{1,2}(x) \equiv \phi(x)$ for symmetric solutions obeys the stationary equation

$$(\mu+1)\phi = -\frac{1}{2}\frac{d^2\phi}{dx^2} + g\phi^3 - \phi(x)\int_{-\infty}^{+\infty}\left[\frac{1}{(b^2+|x-x'|^2)^{3/2}} - \frac{1-3\cos^2\theta}{2(a^2+|x-x'|^2)^{3/2}}\right]\phi^2(x')dx', \quad (2)$$

where $\kappa = G_{\rm DD} = 1$ is fixed, as stated above. Equations (1) and (2) are solved below by means of numerical methods.

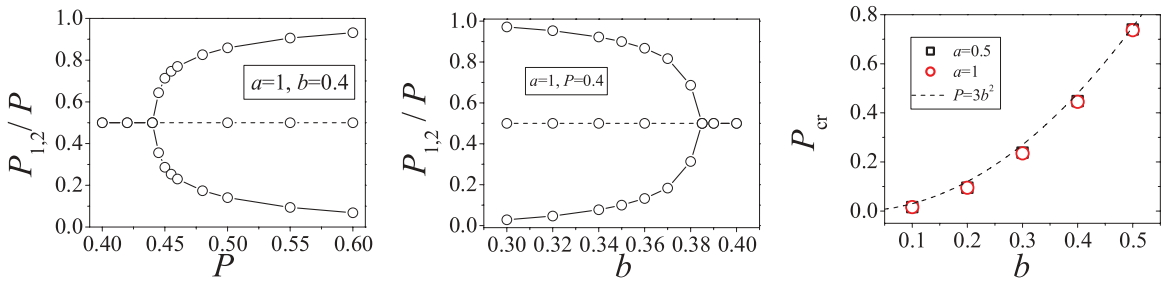

FIG. 3. (Color online) (a) Bifurcation diagram for solitons in the weakly coupled system: The soliton's asymmetry, measured by the deviation of the share of the total power in one core (P_1/P) from 0.5, versus total norm P. (b) Bifurcation diagram as a function of the pipes' diameter b. The circles located along the solid and dashed lines represent stable and unstable solutions, respectively. (c) Critical value of the total norm at the symmetry-breaking point as a function of b for fixed $a = 1$. Stable asymmetric solitons exist above the curve, while the symmetric solitons are stable below it. The curve is well fitted by $P_{cr} = 3b^2$.

In particular, stationary solutions are found below by means of the imaginary-time-propagation method [66] with periodic boundary condition, while the stability of the solutions is tested by means of integration in real time.

B. Weakly coupled system ($a > b$)

Typical examples of stable symmetric, asymmetric, and antisymmetric solitons found in the system represented by Fig. 1(a) are displayed in Fig. 2. Naturally, the asymmetric solitons, morphed by the stronger nonlinearity, are narrower and taller than their symmetric counterparts.

It is relevant to mention that, unlike the standard model of the coupler with the local cubic nonlinearity, where symmetric and antisymmetric solitons are available in an obvious exact form and asymmetric solitons can be effectively described by means of the variational approximation [40,67], in the present strongly nonlocal system such an approximation is not practically possible. Nevertheless, some results can be obtained in an approximate analytical form for the present system too [see Eqs. (5) and (6) below].

Before proceeding to the consideration of the transition between the symmetric and asymmetric solitons, we display the stability area of the antisymmetric ones (which do not undergo any antisymmetry-breaking bifurcation), in the plane of (b, P), in Fig. 2(c). The stability boundary may be fitted to the curve

$$P = 7b^3. \tag{3}$$

Unstable antisymmetric solitons gradually decay into radiation (not shown here in detail).

The SSB for solitons is summarized in Fig. 2 by means of the bifurcation diagrams, which clearly show that the symmetry-breaking bifurcation, driven by the nonlocal attractive DDIs, is supercritical, in contrast to the commonly known subcritical bifurcation in the coupler with the local self-focusing nonlinearity [39,40]. A trend similar to the change of the character of the SSB bifurcation for solitons from subcritical to supercritical, with an increase of the degree of the nonlocality, was recently demonstrated in a model of the optical coupler with weakly nonlocal thermal nonlinearity [59].

As seen from the structure of the first term in the integrand of Eq. (1), a decrease of the diameter b of the parallel pipes implies effective enhancement of the nonlinearity. This, as well as the direct strengthening of the nonlinearity due to an increase of the total norm P, leads to symmetry breaking, as seen in Figs. 3(b) and 3(a). Further, Fig. 3(c) demonstrates the related effect of a decrease of the critical value P_{cr} of the total norm at the bifurcation point with a decrease of b. The latter dependence may be fitted to the formula $P_{cr} = 3b^2$, which is explained by the fact that, at small b, the nearly diverging first integral term in Eq. (2) may be estimated as A^2/b, where A is the soliton's amplitude. Its balance with other terms in the equation leads to estimates for scalings of the amplitude and width:

$$A \sim P/b, \quad W \sim b^2/P. \tag{4}$$

Then, as the SSB point is determined by the competition between the nonlinear intracore and linear intercore-coupling terms in Eq. (1) [39,68,69], the corresponding scaling for the value of P at the critical point indeed takes the form

$$P_{cr} \sim \sqrt{\kappa} b^2 \tag{5}$$

(here κ is kept for clarity, although it was actually scaled to be $\kappa \equiv 1$).

Note that, according to Eq. (3), the stability region for antisymmetric solitons is much smaller at small b. This agrees with the general trend of the antisymmetric solitons in nonlinear couplers to be more fragile modes than their symmetric counterparts [39,47,48] due to the obvious fact that they correspond to a larger coupling energy. In fact, the cubic scaling in Eq. (3) may be qualitatively explained too, although in a more vague form than Eq. (5). Indeed, the antisymmetric soliton with amplitude A is subject to an oscillatory instability characterized by complex growth rates (eigenvalues) $\lambda = \pm i\kappa + \mathrm{Re}\,(\lambda)$, where, in the generic case, an estimate $\mathrm{Re}\,(\lambda) \sim A$ is valid (see, e.g., Ref. [48]). Because the instability is oscillatory, the corresponding perturbations tend to escape from the region of width W, occupied by the soliton [see Eq. (4)], within time $\tau \sim W/V_{gr}$, where the group velocity is determined by the characteristic wave number of the perturbation mode $k \sim W^{-1}$, i.e., $\tau \sim W^2$. The instability accounted for by the escaping perturbations

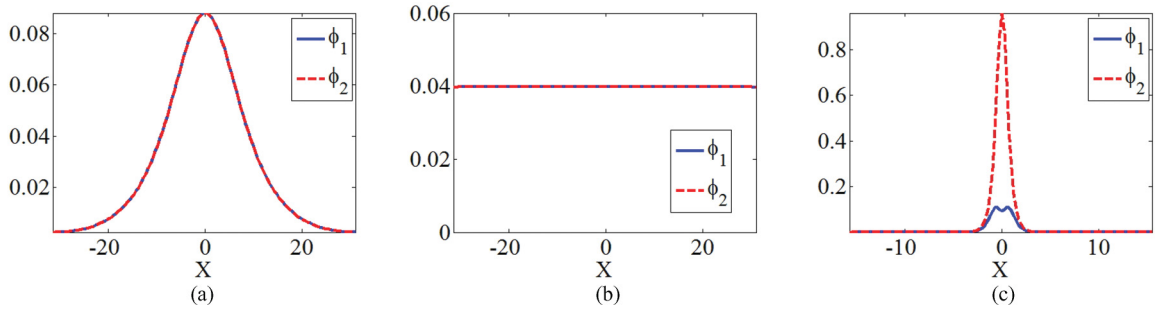

FIG. 4. (Color online) Examples of stable modes found in the strongly coupled system. (a) A symmetric soliton with parameters $(a,b,P) = (0.3,0.5,0.2)$. (b) A symmetric flat state with $(a,b,P) = (0.1,0.5,0.2)$. (c) An asymmetric soliton with $(a,b,P) = (0.2,0.5,1)$.

seems to be convective, which means that it will have enough time to destroy the antisymmetric soliton under condition $\mathrm{Re}\,(\lambda)\,\tau \sim 1$, i.e., according to the above estimates,

$$AW^2 \sim b^3/P \sim 1, \tag{6}$$

which qualitatively explains the numerically found fit (3).

It is also worth noting that additional analysis demonstrates that, as strongly suggested by Figs. 2(d) and 3(c), the general picture of the SSB, being sensitive to the value of b, shows little dependence on the separation between the cores a (in the case of $a > b$, which is considered here). In other words, the SSB in the weakly coupled system, in accordance with its name, is weakly sensitive to the DDI between the parallel cores, which renders the picture relatively simple.

C. Strongly coupled system ($a < b$)

In the setting displayed in Fig. 1(b), the small separation between the effective cores makes the effects of the intercore DDIs essentially stronger compared with the weakly coupled system. In fact, the strongly coupled system realizes an example of competing interactions, namely, intracore attraction and intercore repulsion. A somewhat similar example is the discrete Salerno model with competing signs of the on-site and intersite cubic nonlinearities, which was studied in 1D and 2D settings [70].

The numerical solution demonstrates that, in addition to symmetric and asymmetric solitons, stable flat states with unbroken symmetry between the cores also exist in the strongly coupled system, being stabilized by the strong dipolar repulsion between the cores. A typical example of such stable states is displayed in Fig. 4.

In comparison to their counterparts in the weakly coupled system (cf. Fig. 2), the symmetric solitons are wider in the case of strong coupling. This is also an effect of the repulsive DDI between the cores, which partly cancels the intracore attraction, which forms the symmetric modes. The transition to the asymmetric soliton occurs, as before, with an increase of the total norm, the difference from the weakly coupled system being that the smaller component of the asymmetric mode displays the split-peak structure in Fig. 4(b). This feature originates from the anisotropy [i.e., the θ dependence in the second term in the integrand of Eq. (1)] of the DDI between the cores.

The results of the systematic analysis of the strongly coupled system are summarized in Figs. 5(a) and 5(b) in the form of stability diagrams for all three types of the modes, in the plane of (a,P), for two different fixed values of b. There are two bistability areas where the stable flat state and asymmetric solitons coexist [the large yellow triangular and trapezoidal regions in Figs. 5(a) and 5(b), respectively] or the symmetric and asymmetric solitons are simultaneously stable

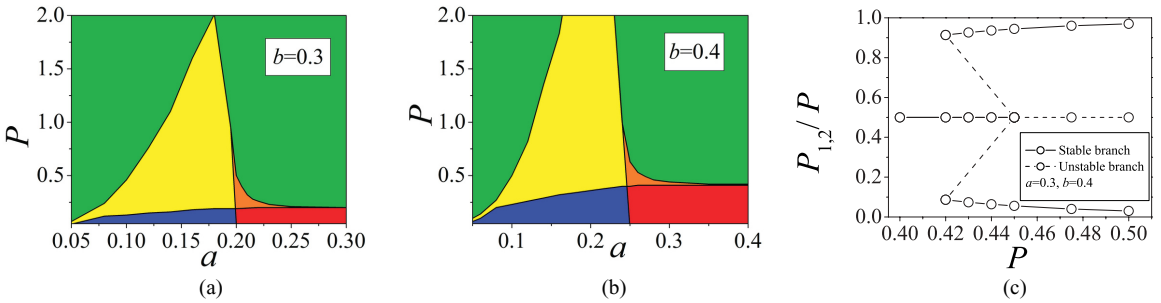

FIG. 5. (Color online) (a) and (b) Stability diagrams in the plane of the total norm P and separation a between the cores of the strongly coupled system for two different values of the overall diameter b. Symmetric solitons are stable in the bottom right red areas, flat states are in the bottom left blue areas, and asymmetric solitons are in the green top areas on the left and right sides. The middle-left yellow areas are regions of the bistability area of the flat state and asymmetric solitons, while the small orange areas at the right center harbor the bistability of the symmetric and asymmetric solitons. (c) Bifurcation diagram for solitons in the strongly coupled system: The soliton's asymmetry, measured by the deviation of the share of the total power in one core (P_1/P) from 0.5, versus total norm P. The type of the symmetry-breaking bifurcation is subcritical here. The dashed segments, which link the stable asymmetric branches and the stable symmetric one, designate the actually missing unstable branches, which, as usual [57], could not be found by means of the imaginary-time-integration method.

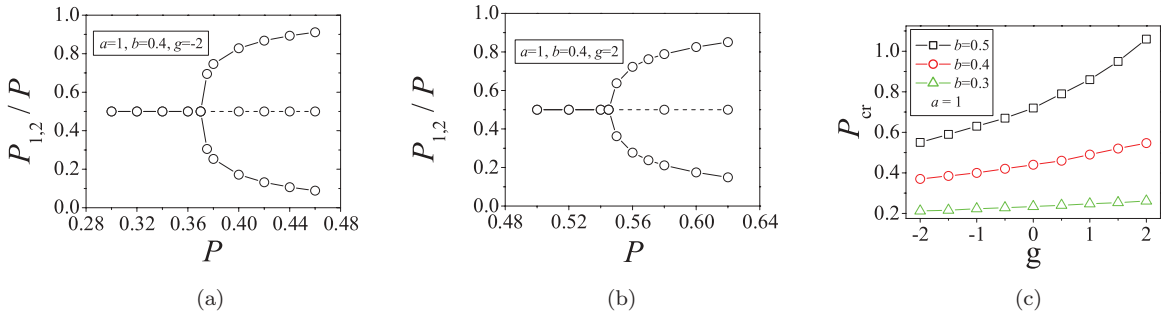

FIG. 6. (Color online) Bifurcation diagrams in the weakly coupled system, with $(a,b) = (1,0.4)$, in the presence of the (a) self-attractive $g = -2$ or (b) self-repulsive $g = 2$ local nonlinearity. (c) Total norm at the bifurcation point as a function of strength g of the additional contact nonlinearity at different fixed values of b.

[small orange regions in Figs. 5(a) and 5(b), respectively]. The presence of the latter bistability area implies that the SSB transition between the symmetric and asymmetric solitons is subcritical in the strongly coupled system, as explicitly shown in the bifurcation diagram in Fig. 5(c) [cf. Fig. 3(a)]. It is thus concluded that the repulsive DDI between the cores plays an increasingly more important role with a decrease of the separation between them a, which becomes the dominant parameter of the system at $a \lesssim (2/3)b$. In particular, only in this region may the symmetric flat state be stable. In contrast, the effect of parameter a is inconspicuous at $a > (2/3)b$, like in the weakly coupled system (see Sec. II B). Accordingly, at $a \to b$, the area of the bistability between the symmetric and asymmetric solitons [the small orange areas in Figs. 5(a) and 5(b)] shrinks to zero, which demonstrates that the SSB changes to the supercritical type, like in the weakly couple case. Finally, antisymmetric solitons and flat states can also be found as stationary solutions of the strongly coupled system, but both these species of the modes turn out to be completely unstable.

D. Effects of local nonlinearity

The inclusion of the local self-attractive ($g < 0$) or self-repulsive ($g > 0$) nonlinearity in the coupled GPEs [Eq. (1)] shifts the point of the SSB bifurcation (the critical value of the total power $P_{\rm cr}$), but it does not change the supercritical character of the bifurcation in the weakly coupled system. The bifurcation diagrams for the system of this type, in the presence of the local nonlinearity of either sign, are presented in Figs. 6(a) and 6(b) (cf. Fig. 3). In addition, Fig. 6(c) displays the dependence of the bifurcation point $P_{\rm cr}$ on the strength g of the local nonlinearity. Naturally, the latter dependence is weaker for smaller values of the pipes' diameter b, as the DDI is stronger at smaller b, suppressing the effect of the local nonlinearity. It is natural too that the self-attractive local nonlinearity ($g < 0$) makes $P_{\rm cr}$ smaller, while the local self-repulsion ($g > 0$) makes it larger. Similarly, the addition of the contact nonlinearity does not change the type of SSB bifurcation in the strongly coupled system either (not shown here in detail).

III. MOBILITY AND COLLISIONS BETWEEN SOLITONS

Collisions between solitons represent an important aspect of the dynamics of integrable and nonintegrable models [71]. In dual-core systems, one can study collisions between symmetric solitons and, most interestingly, between asymmetric solitons with equal or opposite polarities, i.e., with larger components belonging to the same or different cores [72]. These three cases are schematically defined in Fig. 7.

We report here numerical results for collisions between solitons in the weakly coupled system, taking the initial state at $t = 0$ as a pair of widely separated kicked solitons,

$$\psi_{1,2}^{(0)} = U_{1,2}^{(1)}(x + x_0, P)e^{i\eta(x+x_0)} + U_{1,2}^{(2)}(x - x_0, P)e^{-i\eta(x-x_0)}, \tag{7}$$

where $U_{1,2}^{(1,2)}(x \pm x_0, P)$ are the two-component soliton solutions with total powers P, which are centered at $x = \mp x_0$ with sufficiently large initial separation $2x_0$, and η is the kick (momentum imparted to the soliton). Solutions $U^{(1)}$ and $U^{(2)}$ are either identical or, in the above-mentioned case of opposite polarities, two asymmetric solitons with swapped components [see Fig. 7(b)].

In Figs. 8 and 9 we display typical results of collisions for asymmetric soliton pairs in the case that is close to

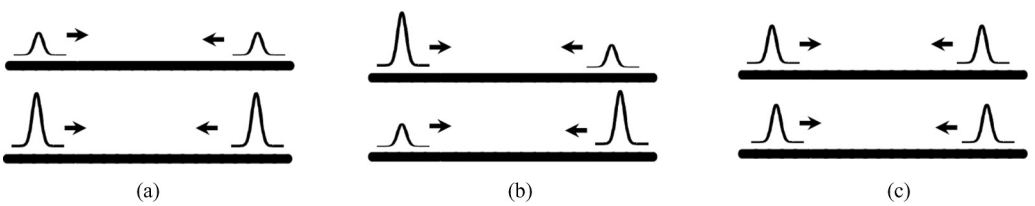

FIG. 7. Three types of collisions between solitons in the dual-core system: (a) unipolar asymmetric solitons with the larger components belonging to the same core, (b) asymmetric solitons with opposite polarities, and (c) symmetric solitons.

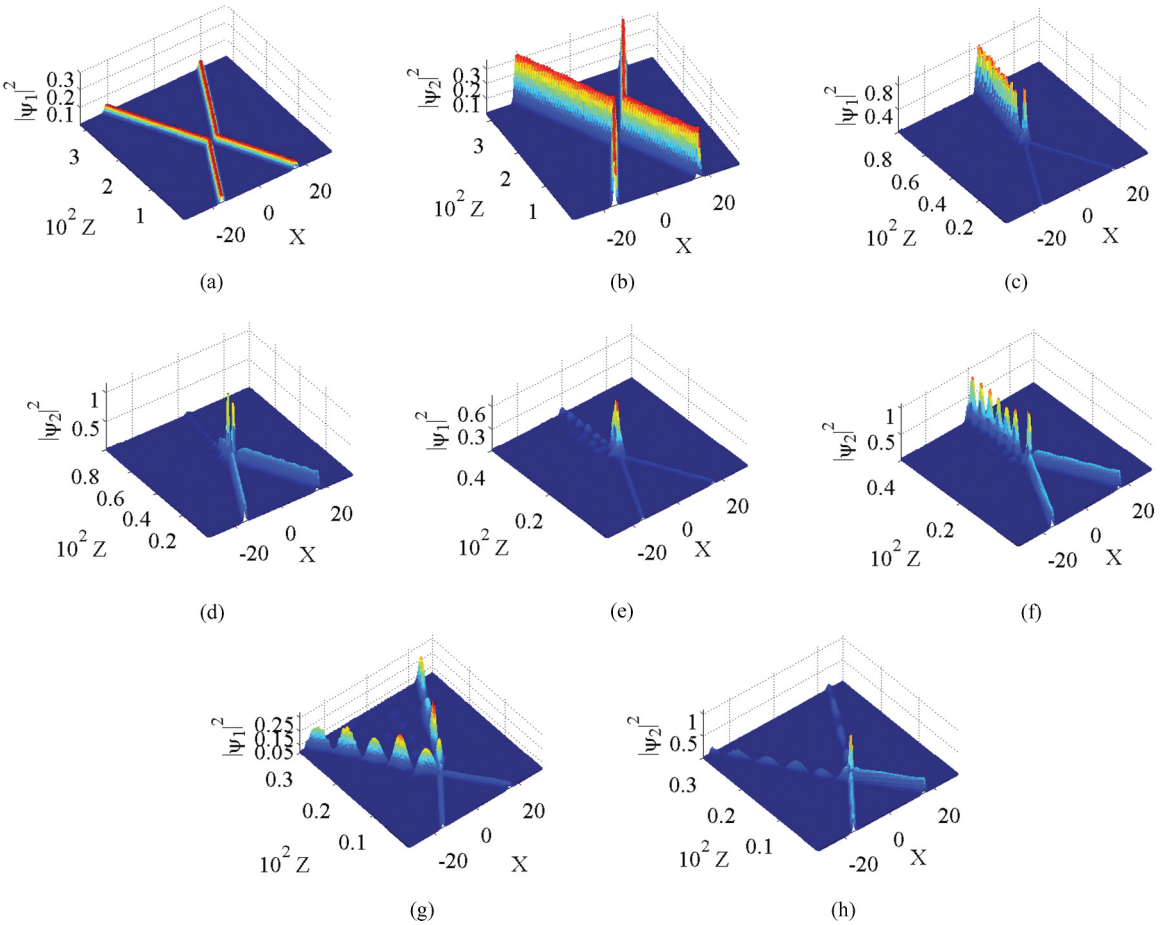

FIG. 8. (Color online) Examples of collisions between unipolar asymmetric solitons for (a) and (b) slow solitons with $\eta = 0.1$, (c) and (d) intermediate velocity $\eta = 0.4$, (e) and (f) larger intermediate velocity $\eta = 0.8$, and (g) and (h) fast solitons with $\eta = 1.6$.

the border between the weakly and strongly bound systems $(a,b,P) = (1,0.4,0.5)$. Figures 8(a), 8(b), 9(a), and 9(b) show that slowly moving solitons bounce back from each other elastically. When the kick and ensuing velocities are larger,

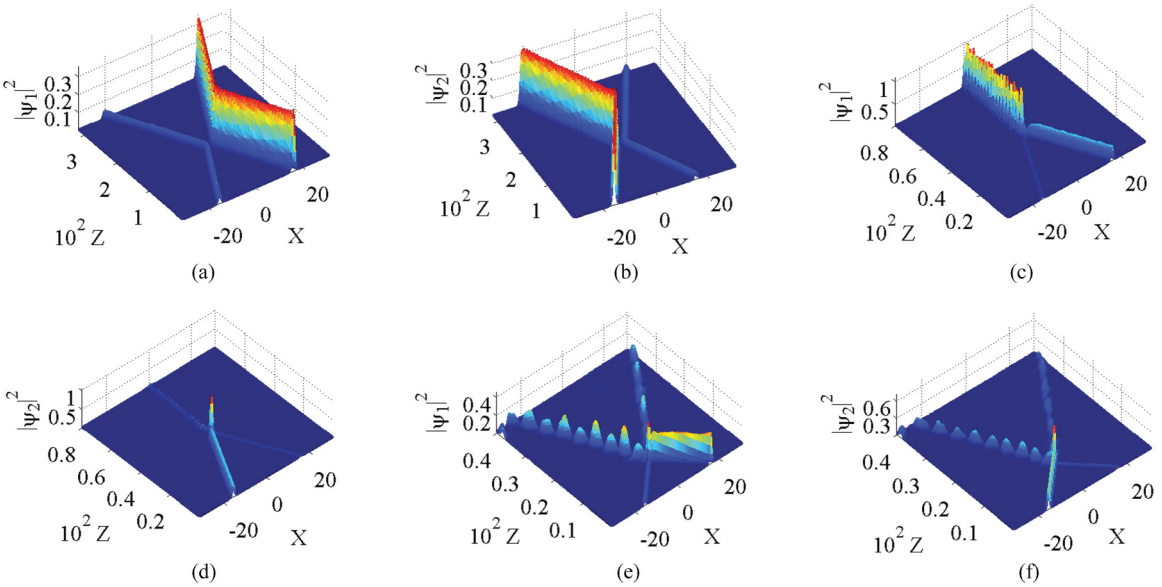

FIG. 9. (Color online) Examples of collisions between asymmetric solitons with opposite polarities for (a) and (b) slow solitons with $\eta = 0.1$, (c) and (d) intermediate velocity $\eta = 0.4$, and (e) and (f) fast solitons with $\eta = 1.6$.

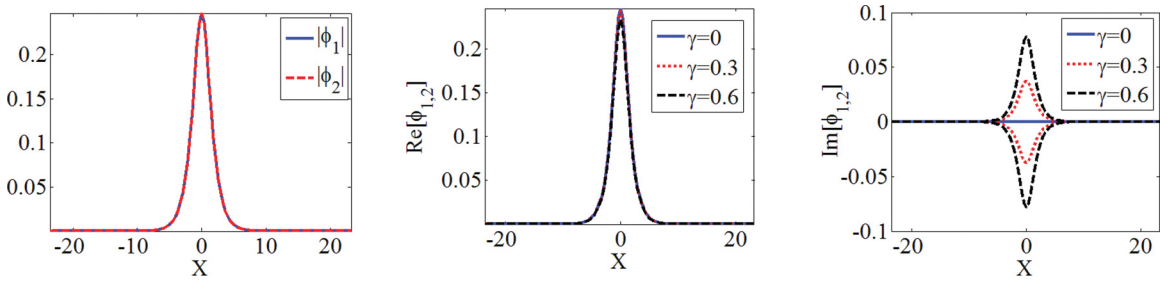

FIG. 10. (Color online) Examples of stable $\mathcal{PT}$-symmetric solitons, defined as per Eq. (9), with $(a,b,P) = (1,0.4,0.3)$ for $\gamma = 0$, 0.3, and 0.6. (a) Profile of $|\psi_{1,2}(x)|$, which is common for the three solitons. (b) Real and (c) imaginary parts of the solitons.

the collision becomes inelastic, leading to the merger of the solitons into a single asymmetric breather. Figures 8(c)–8(f) demonstrate that the merger of the colliding unipolar solitons may switch the polarity of the emerging breather from that of the original solitons or produce a breather that keeps the original polarity. The merger of the solitons with opposite polarities gives rise to an asymmetric breather whose polarity is established spontaneously, as seen in Figs. 9(c) and 9(d). Finally, at still larger values of the kick, the moving solitons pass through each other, reappearing in an excited form (each one as a moving breather) [see Figs. 8(g), 8(h), 9(e), and 9(f)]. The norms of the outgoing vibrating solitons are equal, as they were before the collision.

The same sequence of outcomes of the collisions—rebound, merger into a breather, and passage in the form of moving breathers—is observed, with an increase of the kick η, at other values of the parameters. Collisions between symmetric solitons seem simpler (not shown here in detail): rebound at small values of η and passage, without conspicuous excitation of intrinsic vibrations, at larger η.

IV. THE $\mathcal{PT}$-SYMMETRIC VERSION OF THE WEAKLY COUPLED SYSTEM

The realization of $\mathcal{PT}$-symmetric systems in BECs was proposed by linearly coupling two traps (cores, in the present terms) with the loss of atoms in one trap and the gain of atoms in the other, which may be provided by a matter-wave laser [73]. The objective of the analysis was to provide a direct realization of the $\mathcal{PT}$ symmetry in quantum media, after it was proposed [74] and implemented [75] in classical optics (see also Ref. [76]).

Accordingly, the $\mathcal{PT}$-balanced version of linearly coupled GPEs (1) is

$$
\begin{aligned}
i\frac{\partial\psi_1}{\partial t} &= -\frac{1}{2}\frac{\partial^2\psi_1}{\partial x^2} - \psi_2 + i\gamma\psi_1 \\
&\quad - \psi_1\int_{-\infty}^{+\infty}\left[\frac{|\psi_1(x')|^2}{(b^2+|x-x'|^2)^{3/2}} - \frac{1}{2}(1-3\cos^2\theta)\right. \\
&\quad \left.\times\frac{|\psi_2(x')|^2}{(a^2+|x-x'|^2)^{3/2}}\right]dx', \\
i\frac{\partial\psi_2}{\partial t} &= -\frac{1}{2}\frac{\partial^2\psi_2}{\partial x^2} - \psi_1 - i\gamma\psi_2 \\
&\quad - \psi_2\int_{-\infty}^{+\infty}\left[\frac{|\psi_2(x')|^2}{(b^2+|x-x'|^2)^{3/2}} - \frac{1}{2}(1-3\cos^2\theta)\right. \\
&\quad \left.\times\frac{|\psi_1(x')|^2}{(a^2+|x-x'|^2)^{3/2}}\right]dx',
\end{aligned}
\tag{8}
$$

where $\gamma > 0$ is the coefficient of the gain and loss in the first and second cores, respectively, $\kappa = G_{\rm DD} \equiv 1$ is fixed, as above, and the local nonlinearity is dropped ($g = 0$). As in the recently studied model of the $\mathcal{PT}$-symmetric coupler with cubic nonlinearity [47,48], stationary $\mathcal{PT}$-symmetric and -antisymmetric solutions to Eq. (8) can be found as

$$
\psi_{1,2}^{(\rm symm)}(x,t) = e^{-i\mu t}\phi(x)\exp\left(\pm\tfrac{1}{2}i\arcsin\gamma\right) \equiv e^{-i\mu t}\phi_{1,2}(x), \tag{9}
$$

$$
\psi_{1,2}^{(\rm anti)}(x,t) = \pm ie^{-i\mu t}\phi(x)\exp\left(\mp\tfrac{1}{2}i\arcsin\gamma\right), \tag{10}
$$

where the upper and lower signs correspond to subscripts 1 and 2, respectively, μ is a real chemical potential, and the real function $\phi(x)$ is the solution of the stationary equation (2) for symmetric solitons in the system without the $\mathcal{PT}$ terms and with the same value of μ. Obviously, the symmetric and

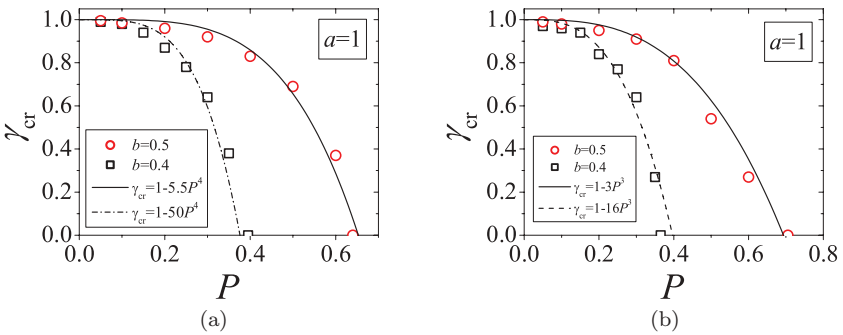

FIG. 11. (Color online) Critical value $\gamma_{\rm cr}$ (the stability boundary for the $\mathcal{PT}$-symmetric solitons) versus the total norm P at different fixed values of the pipe's parameter b in the weakly coupled system for (a) symmetric solitons (9) and (b) antisymmetric solitons (10). The continuous and dashed curves are guides for the eye.

antisymmetric solitons exist for $\gamma < 1$ and form continuous families parametrized by μ, like their counterparts in the conservative system.

Here we focus on the analysis of the stability of the $\mathcal{PT}$-symmetric and -antisymmetric solitons (9), which is a nontrivial problem in the present context. Typical examples of stable symmetric solitons are displayed in Fig. 10, along with their counterpart in the system without the $\mathcal{PT}$ terms ($\gamma = 0$).

The $\mathcal{PT}$-symmetric and -antisymmetric solitons remain stable up to a certain critical value $\gamma_{\rm cr}$ of the gain-loss coefficient and are unstable in the interval of $\gamma_{\rm cr} < \gamma < 1$, which is a situation typical for solitons in $\mathcal{PT}$ -symmetric systems [47,48,77]. The unstable solitons suffer a blowup of the pumped component and decay of the damped one, which is a typical scenario too (not shown here in detail). The most essential results are presented in Fig. 11 for the weakly coupled system in the form of the dependence of $\gamma_{\rm cr}$ on the total norm for different diameters of the parallel-coupled pipes b (recall that b was demonstrated above to be the most essential coefficient for the weakly coupled system). The figure demonstrates that the instability region expands as the nonlinear interactions get stronger, which is caused by either an increase of the total norm P or a decrease of b.

V. CONCLUSION

The objective of this work was to extend the study of the symmetry breaking of solitons in dual-core systems with the cubic nonlinearity and linear coupling between the cores, which has been previously analyzed in full detail for local interactions, to dipolar BECs with long-range interactions, which act both inside each core and between them. Two versions of the system were introduced, weakly and strongly coupled ones, depending on the relation between the diameter of the pipe-shaped traps and the distance between them. In either case, the linear coupling accounts for hopping of atoms between the cores. The symmetry-breaking bifurcation and stability regions for symmetric and asymmetric solitons, as well as for nonbifurcating antisymmetric solitons, have been identified in both systems. In addition to the solitons, the strongly coupled system supports a stability region for flat states with unbroken symmetry between the cores due to the competition between the attractive and repulsive intracore and intercore dipole-dipole interactions. Collisions between kicked asymmetric solitons in the weakly coupled system were systematically studied too, showing bouncing back at small velocities, a merger into an asymmetric breather in the intermediate range, and the reappearance of vibrating fast solitons after the collision. Finally, a $\mathcal{PT}$-symmetric generalization of the weakly coupled system was introduced as a more exotic extension of the system and a stability boundary for $\mathcal{PT}$-symmetric and -antisymmetric solitons was found. A challenging generalization of the analysis may be its application to 2D dual-core systems, where in particular the symmetry breaking may occur not only for fundamental solitons, but also for solitary vortices.

ACKNOWLEDGMENTS

We appreciate a valuable discussion with L. Santos. This work was supported by the Chinese agency CNNSF (Grants No. 11104083, No. 11204089, and No. 11205063), the Guangdong Provincial Science and Technology Projects No. 2011B090400325, the German-Israel Foundation through Grant No. I-1024-2.7/2009, and the Tel Aviv University in the framework of the matching scheme for the postdoctoral fellowship of Y.L.

[1] A. Griesmaier, J. Phys. B **40**, R91 (2007).

[2] T. Lahaye, C. Menotti, L. Santos, M. Lewenstein, and T. Pfau, Rep. Prog. Phys. **72**, 126401 (2009).

[3] M. Baranov, L. Dobrek, K. Goral, L. Santos, and M. Lewenstein, Phys. Scr., T **102**, 74 (2002); M. A. Baranov, Phys. Rep. **464**, 71 (2008).

[4] H. Saito, Y. Kawaguchi, and M. Ueda, Phys. Rev. Lett. **102**, 230403 (2009); R. Nath and L. Santos, Phys. Rev. A **81**, 033626 (2010); A. Bühler and H. P. Büchler, *ibid.* **84**, 023607 (2011); A. Maluckov, G. Gligorić, Lj. Hadžievski, B. A. Malomed, and T. Pfau, Phys. Rev. Lett. **108**, 140402 (2012).

[5] M. Klawunn and L. Santos, Phys. Rev. A **80**, 013611 (2009); K. Łakomy, R. Nath, and L. Santos, *ibid.* **86**, 023620 (2012).

[6] R. Richter and I. V. Barashenkov, Phys. Rev. Lett. **94**, 184503 (2005).

[7] S. Müller, J. Billy, E. A. L. Henn, H. Kadau, A. Griesmaier, M. Jona-Lasinio, L. Santos, and T. Pfau, Phys. Rev. A **84**, 053601 (2011).

[8] R. M. Wilson, S. Ronen, J. L. Bohn, and H. Pu, Phys. Rev. Lett. **100**, 245302 (2008); R. M. Wilson and J. L. Bohn, Phys. Rev. A **83**, 023623 (2011); C. Ticknor, R. M. Wilson, and J. L. Bohn, Phys. Rev. Lett. **106**, 065301 (2011); D. Hufnagl, R. Kaltseis, V. Apaja, and R. E. Zillich, *ibid.* **107**, 065303 (2011).

[9] K. Gawryluk, K. Bongs, and M. Brewczyk, Phys. Rev. Lett. **106**, 140403 (2011).

[10] M. Lu, S. H. Youn, and B. L. Lev, Phys. Rev. Lett. **104**, 063001 (2010); M. Lu, N. Q. Burdick, S. H. Youn, and B. L. Lev, *ibid.* **107**, 190401 (2011).

[11] J. J. McClelland and J. L. Hanssen, Phys. Rev. Lett. **96**, 143005 (2006); K. Aikawa, A. Frisch, M. Mark, S. Baier, A. Rietzler, R. Grimm, and F. Ferlaino, *ibid.* **108**, 210401 (2012).

[12] M. A. Baranov, M. S. Mar'enko, V. S. Rychkov, and G. V. Shlyapnikov, Phys. Rev. A **66**, 013606 (2002); M. A. Baranov, L. Dobrek, and M. Lewenstein, Phys. Rev. Lett. **92**, 250403 (2004); M. A. Baranov, K. Osterloh, and M. Lewenstein, *ibid.* **94**, 070404 (2005); A. Micheli, G. Pupillo, H. P. Büchler, and P. Zoller, Phys. Rev. A **76**, 043604 (2007); T. Miyakawa, T. Sogo, and H. Pu, *ibid.* **77**, 061603 (2008); G. M. Bruun and E. Taylor, Phys. Rev. Lett. **101**, 245301 (2008); B. M. Fregoso, K. Sun, E. Fradkin, and B. L. Lev, New J. Phys. **11**, 103003 (2009); T. Sogo, L. He, T. Miyakawa, S. Yi, H. Lu, and H. Pu, *ibid.* **11**, 055017 (2009); B. M. Fregoso and E. Fradkin,

Phys. Rev. Lett. **103**, 205301 (2009); M. Lu, S. H. Youn, and B. L. Lev, *ibid.* **104**, 063001 (2010).
[13] D. Jaksch and P. Zoller, Ann. Phys. (N.Y.) **315**, 52 (2005); I. Bloch, J. Dalibard, and S. Nascimbène, Nat. Phys. **8**, 267 (2012); A. A. Houck, H. E. Türeci, and J. Koch, *ibid.* **8**, 292 (2012); P. Hauke, F. M. Cucchietti, L. Tagliacozzo, I. Deutsch, and M. Lewenstein, Rep. Prog. Phys. **75**, 082401 (2012).
[14] M. Lewenstein, A. Sanpera, and V. Ahufinger, *Ultracold Atoms in Optical Lattices* (Oxford University Press, Oxford, 2012).
[15] A. G. Litvak, V. A. Mironov, G. M. Fraiman, and A. D. Yunakovskii, Sov. J. Plasma Phys. **1**, 31 (1975).
[16] C. Conti, M. Peccianti, and G. Assanto, Phys. Rev. Lett. **91**, 073901 (2003); M. Peccianti, C. Conti, G. Assanto, A. D. Luca, and C. Umeton, Nature (London) **432**, 733 (2004).
[17] W. Królikowski, O. Bang, J. J. Rasmussen, and J. Wyller, Phys. Rev. E **64**, 016612 (2001); O. Bang, W. Królikowski, J. Wyller, and J. J. Rasmussen, *ibid.* **66**, 046619 (2002); W. Królikowski, O. Bang, J. J. Rasmussen, and J. Wyller, Opt. Express **13**, 435 (2005); C. Rotschild, B. Alfassi, O. Cohen, and M. Segev, Nat. Phys. **2**, 769 (2006); A. Dreischuh, D. N. Neshev, D. E. Petersen, O. Bang, and W. Królikowski, Phys. Rev. Lett. **96**, 043901 (2006).
[18] E. A. Ultanir, G. I. Stegeman, D. Michaelis, C. H. Lange, and F. Lederer, Phys. Rev. Lett. **90**, 253903 (2003).
[19] D. O'Dell, S. Giovanazzi, G. Kurizki, and V. M. Akulin, Phys. Rev. Lett. **84**, 5687 (2000); S. Giovanazzi, D. O'Dell, and G. Kurizki, Phys. Rev. A **63**, 031603 (2001); I. Papadopoulos, P. Wagner, G. Wunner, and J. Main, *ibid.* **76**, 053604 (2007).
[20] S. Sinha and L. Santos, Phys. Rev. Lett. **99**, 140406 (2007); J. Cuevas, B. A. Malomed, P. G. Kevrekidis, and D. J. Frantzeskakis, Phys. Rev. A **79**, 053608 (2009).
[21] G. Gligorić, A. Maluckov, L. Hadžievski, and B. A. Malomed, Phys. Rev. A **78**, 063615 (2008); **79**, 053609 (2009); J. Phys. B **42**, 145302 (2009).
[22] B. B. Baizakov, F. Kh. Abdullaev, B. A. Malomed, and M. Salerno, J. Phys. B **42**, 175302 (2009).
[23] L. Salasnich, B. A. Malomed, and F. Toigo, Phys. Rev. A **77**, 035601 (2008).
[24] L. E. Young-S., P. Muruganandam, and S. K. Adhikari, J. Phys. B **44**, 101001 (2011).
[25] P. Muruganandam and S. K. Adhikari, J. Phys. B **44**, 121001 (2011).
[26] G. Gligorić, A. Maluckov, M. Stepić, L. Hadžievski, and B. A. Malomed, Phys. Rev. A **81**, 013633 (2010); J. Phys. B **43**, 055303 (2010).
[27] P. Pedri and L. Santos, Phys. Rev. Lett. **95**, 200404 (2005).
[28] I. Tikhonenkov, B. A. Malomed, and A. Vardi, Phys. Rev. A **78**, 043614 (2008).
[29] S. Giovanazzi, A. Görlitz, and T. Pfau, Phys. Rev. Lett. **89**, 130401 (2002).
[30] V. M. Lashkin, Phys. Rev. A **75**, 043607 (2007).
[31] I. Tikhonenkov, B. A. Malomed, and A. Vardi, Phys. Rev. Lett. **100**, 090406 (2008); P. Köberle, D. Zajec, G. Wunner, and B. A. Malomed, Phys. Rev. A **85**, 023630 (2012).
[32] R. Eichler, J. Main, and G. Wunner, Phys. Rev. A **83**, 053604 (2011).
[33] P. Antonelli and C. Sparber, Physica D **240**, 426 (2011).
[34] R. Nath, P. Pedri, and L. Santos, Phys. Rev. Lett. **102**, 050401 (2009).
[35] M. Greiner, O. Mandel, T. Esslinger, T. W. Hansch, and I. Bloch, Nature (London) **415**, 39 (2002).
[36] R. Nath, P. Pedri, and L. Santos, Phys. Rev. A **76**, 013606 (2007).
[37] K. Łakomy, R. Nath, and L. Santos, Phys. Rev. A **86**, 013610 (2012).
[38] K. Łakomy, R. Nath, and L. Santos, Phys. Rev. A **85**, 033618 (2012).
[39] S. Trillo, S. Wabnitz, E. M. Wright, and G. I. Stegeman, Opt. Lett. **13**, 672 (1988); S. R. Friberg, A. M. Weiner, Y. Silberberg, B. G. Sfez, and P. S. Smith, *ibid.* **13**, 904 (1988); F. Kh. Abdullaev, R. M. Abrarov, and S. A. Darmanyan, *ibid.* **14**, 131 (1989); S. Trillo, S. Wabnitz, E. M. Wright, and G. I. Stegeman, Opt. Commun. **70**, 166 (1989); E. M. Wright, G. I. Stegeman, and S. Wabnitz, Phys. Rev. A **40**, 4455 (1989); M. Romagnoli, S. Trillo, and S. Wabnitz, Opt. Quantum Electron. **24**, S1237 (1992); N. Akhmediev and A. Ankiewicz, Phys. Rev. Lett. **70**, 2395 (1993); J. M. Soto-Crespo and N. Akhmediev, Phys. Rev. E **48**, 4710 (1993); K. S. Chiang, Opt. Lett. **20**, 997 (1995); A. Mostofi, B. A. Malomed, and P. L. Chu, Opt. Commun. **145**, 274 (1998).
[40] C. Paré and M. Fłorjańczyk, Phys. Rev. A **41**, 6287 (1990); A. I. Maimistov, Kvant. Elektron. **18**, 758 (1991) [Sov. J. Quantum Electron. **21**, 687 (1991)]; P. L. Chu, B. A. Malomed, and G. D. Peng, J. Opt. Soc. Am. B **10**, 1379 (1993); B. A. Malomed, I. M. Skinner, P. L. Chu, and G. D. Peng, Phys. Rev. E **53**, 4084 (1996); H. Sakaguchi and B. A. Malomed, *ibid.* **83**, 036608 (2011); Y. Li, B. A. Malomed, M. Feng, and J. Zhou, Phys. Rev. A **83**, 053832 (2011); Y. Li, W. Pang, and B. A. Malomed, *ibid.* **86**, 023832 (2012).
[41] B. A. Malomed, Phys. Rev. E **50**, 1565 (1994); N. Dror, B. A. Malomed, and J. Zeng, *ibid.* **84**, 046602 (2011).
[42] W. C. K. Mak, B. A. Malomed, and P. L. Chu, J. Opt. Soc. Am. B **15**, 1685 (1998); Phys. Rev. E **69**, 066610 (2004); S. Ha, A. A. Sukhorukov, and Y. S. Kivshar, Opt. Lett. **32**, 1429 (2007); Y. J. Tsofe and B. A. Malomed, Phys. Rev. E **75**, 056603 (2007); S. Ha and A. A. Sukhorukov, J. Opt. Soc. Am. B **25**, C15 (2008).
[43] G. Herring, P. G. Kevrekidis, B. A. Malomed, R. Carretero-González, and D. J. Frantzeskakis, Phys. Rev. E **76**, 066606 (2007); Lj. Hadžievski, G. Gligorić, A. Maluckov, and B. A. Malomed, Phys. Rev. A **82**, 033806 (2010).
[44] W. C. K. Mak, B. A. Malomed, and P. L. Chu, Phys. Rev. E **55**, 6134 (1997); **57**, 1092 (1998).
[45] L. Albuch and B. A. Malomed, Math. Comput. Simul. **74**, 312 (2007); Z. Birnbaum and B. A. Malomed, Physica D **237**, 3252 (2008); P. A. Tsilifis, P. G. Kevrekidis, and V. M. Rothos, arXiv:1207.6731.
[46] A. Sigler, B. A. Malomed, and D. V. Skryabin, Phys. Rev. E **74**, 066604 (2006).
[47] R. Driben and B. A. Malomed, Opt. Lett. **36**, 4323 (2011); Europhys. Lett. **96**, 51001 (2011).
[48] N. V. Alexeeva, I. V. Barashenkov, A. A. Sukhorukov, and Y. S. Kivshar, Phys. Rev. A **85**, 063837 (2012).
[49] R. Ulrich and A. Simon, Appl. Opt. **18**, 2241 (1979); Y. Fujii and K. Sano, *ibid.* **19**, 2602 (1980); A. Mecozzi, S. Trillo, S. Wabnitz, and B. Daino, Opt. Lett. **12**, 275 (1987); M. V. Tratnik and J. E. Sipe, Phys. Rev. A **38**, 2011 (1988); S. Wabnitz, S. Trillo, E. M. Wright, and G. I. Stegeman, J. Opt. Soc. Am. **8**, 602 (1991); A. B. Aceves and S. Wabnitz, Opt. Lett. **17**, 25 (1992); V. S. Liberman and B. Y. Zeldovich, Phys. Rev. A **46**, 5199

(1992); S. F. Feldman, D. A. Weinberger, and H. G. Winful, J. Opt. Soc. Am. B **10**, 1191 (1993); C. R. Menyuk and P. K. A. Wai, *ibid.* **11**, 1288 (1994); E. A. Kuzin, N. Korneev, J. W. Haus, and B. Ibarra-Escamilla, *ibid.* **18**, 919 (2001); C. N. Alexeyev and M. A. Yavorsky, J. Opt. A: Pure Appl. Opt. **6**, 824 (2004).

[50] G. Kakarantzas, A. Ortigosa-Blanch, T. A. Birks, P. S. Russell, L. Farr, F. Couny, and B. J. Mangan, Opt. Lett. **28**, 158 (2003); L. Y. Zang, M. S. Kang, M. Kolesik, M. Scharrer, and P. Russell, J. Opt. Soc. Am. B **27**, 1742 (2010); G. K. L. Wong, M. S. Kang, H. W. Lee, F. Biancalana, C. Conti, T. Weiss, and P. St. J. Russell, Science **337**, 446 (2012).

[51] P. I. D. C. Reyes and P. S. Westbrook, IEEE Photon. Tech. Lett. **15**, 828 (2003); V. I. Kopp, V. M. Churikov, J. Singer, N. Chao, D. Neugroschl, and A. Z. Genack, Science **305**, 74 (2004).

[52] Y. Li, W. Pang, S. Fu, and B. A. Malomed, Phys. Rev. A **85**, 053821 (2012).

[53] A. Gubeskys and B. A. Malomed, Phys. Rev. A **75**, 063602 (2007); **76**, 043623 (2007).

[54] R. J. Ballagh, K. Burnett, and T. F. Scott, Phys. Rev. Lett. **78**, 1607 (1997); A. Kuklov, N. Prokof'ev, and B. Svistunov, Phys. Rev. A **69**, 025601 (2004); J. Williams, R. Walser, J. Cooper, E. Cornell, and M. Holland, *ibid.* **59**, R31 (1999); P. Öhberg and S. Stenholm, *ibid.* **59**, 3890 (1999); D. T. Son and M. A. Stephanov, *ibid.* **65**, 063621 (2002); S. D. Jenkins and T. A. B. Kennedy, *ibid.* **68**, 053607 (2003); Q.-H. Park and J. H. Eberly, *ibid.* **70**, 021602(R) (2004); B. Juliá-Díaz, M. Guilleumas, M. Lewenstein, A. Polls, and A. Sanpera, *ibid.* **80**, 023616 (2009); B. Juliá-Díaz, D. Dagnino, M. Lewenstein, J. Martorell, and A. Polls, *ibid.* **81**, 023615 (2010).

[55] I. M. Merhasin, B. A. Malomed, and R. Driben, J. Phys. B **38**, 877 (2005); S. K. Adhikari and B. A. Malomed, Phys. Rev. A **74**, 053620 (2006); **79**, 015602 (2009).

[56] H. Saito, R. G. Hulet, and M. Ueda, *ibid.* **76**, 053619 (2007); H. Susanto, P. G. Kevrekidis, B. A. Malomed, and F. Kh. Abdullaev, Phys. Lett. A **372**, 1631 (2008).

[57] M. Matuszewski, B. A. Malomed, and M. Trippenbach, Phys. Rev. A **75**, 063621 (2007); M. Trippenbach, E. Infeld, J. Gocalek, M. Matuszewski, M. Oberthaler, and B. A. Malomed, *ibid.* **78**, 013603 (2008); N. V. Hung, M. Trippenbach, and B. A. Malomed, *ibid.* **84**, 053618 (2011).

[58] N. V. Hung, P. Ziń, M. Trippenbach, and B. A. Malomed, Phys. Rev. E **82**, 046602 (2010).

[59] X. Shi, B. A. Malomed, F. Ye, and X. Chen, Phys. Rev. A **85**, 053839 (2012).

[60] A. W. Snyder and D. J. Mitchell, Science **276**, 1538 (1997).

[61] T. Lahaye, T. Pfau, and L. Santos, Phys. Rev. Lett. **104**, 170404 (2010); D. Peter, K. Pawłowski, T. Pfau, and K. Rzażewski, J. Phys. B **45**, 225302 (2012).

[62] R. Bucker, A. Perrin, S. Manz, T. Betz, C. Koller, T. Plisson, J. Rottmann, T. Schumm, and J. Schmiedmayer, New J. Phys. **11**, 103039 (2009).

[63] G. Iooss and D. D. Joseph, *Elementary Stability and Bifurcation Theory* (Springer, New York, 1980).

[64] C. M. Bender, Rep. Prog. Phys. **70**, 947 (2007).

[65] T. Lahaye, T. Koch, B. Froehlich, M. Fattori, J. Metz, A. Griesmaier, S. Giovanazzi, and T. Pfau, Nature (London) **448**, 672 (2007).

[66] M. L. Chiofalo, S. Succi, and M. P. Tosi, Phys. Rev. E **62**, 7438 (2000).

[67] B. A. Malomed, in *Progress in Optics*, edited by E. Wolf (North-Holland, Amsterdam, 2002), Vol. 43, p. 71.

[68] L. Salasnich and B. A. Malomed, Mol. Phys. **109**, 2737 (2011).

[69] A. W. Snyder, D. J. Mitchell, L. Poladian, D. R. Rowland, and Y. Chen, J. Opt. Soc. Am. B **8**, 2102 (1991); A. Mostofi, B. A. Malomed, and P. L. Chu, Opt. Commun. **137**, 244 (1997); J. H. Li, K. S. Chiang, B. A. Malomed, and K. W. Chow, J. Phys. B **45**, 165404 (2012).

[70] J. Gomez-Gardeñes, B. A. Malomed, L. M. Floría, and A. R. Bishop, Phys. Rev. E **73**, 036608 (2006); **74**, 036607 (2006).

[71] J. Yang, *Nonlinear Waves in Integrable and Nonintegrable Systems* (SIAM, Philadelphia, 2010).

[72] G. D. Peng, B. A. Malomed, and P. L. Chu, Phys. Scr. **58**, 1498 (1998); A. Espinosa-Ceròn, B. A. Malomed, J. Fujioka, and R. F. Rodríguez, Chaos **22**, 033145 (2012).

[73] S. Klaiman, U. Günther, and N. Moiseyev, Phys. Rev. Lett. **101**, 080402 (2008); H. Cartarius and G. Wunner, Phys. Rev. A **86**, 013612 (2012).

[74] A. Ruschhaupt, F. Delgado, and J. G. Muga, J. Phys. A **38**, L171 (2005); R. El-Ganainy, K. G. Makris, D. N. Christodoulides, and Z. H. Musslimani, Opt. Lett. **32**, 2632 (2007); M. V. Berry, J. Phys. A **41**, 244007 (2008); K. G. Makris, R. El-Ganainy, D. N. Christodoulides, and Z. H. Musslimani, Phys. Rev. Lett. **100**, 103904 (2008); S. Longhi, *ibid.* **103**, 123601 (2009).

[75] A. Guo, G. J. Salamo, D. Duchesne, R. Morandotti, M. Volatier-Ravat, V. Aimez, G. A. Siviloglou, and D. N. Christodoulides, Phys. Rev. Lett. **103**, 093902 (2009); C. E. Ruter, K. G. Makris, R. El-Ganainy, D. N. Christodoulides, M. Segev, and D. Kip, Nat. Phys. **6**, 192 (2010).

[76] K. G. Makris, R. El-Ganainy, D. N. Christodoulides, and Z. H. Musslimani, Int. J. Theor. Phys. **50**, 1019 (2011).

[77] Z. H. Musslimani, K. G. Makris, R. El-Ganainy, and D. N. Christodoulides, Phys. Rev. Lett. **100**, 030402 (2008); X. Zhu, H. Wang, L.-X. Zheng, H. Li, and Y.-J. He, Opt. Lett. **36**, 2680 (2011); F. Kh. Abdullaev, Y. V. Kartashov, V. V. Konotop, and D. A. Zezyulin, Phys. Rev. A **83**, 041805(R) (2011); S. Nixon, L. Ge, and J. Yang, *ibid.* **85**, 023822 (2012); Y. He, X. Zhu, D. Mihalache, J. Liu, and Z. Chen, *ibid.* **85**, 013831 (2012).